

Searching for Xb state

Gang Li (李刚)

Department of Physics, Qufu Normal University

Ref: G. Li, W. Wang, PLB733, 100 (2014); G. Li, Z. Zhou, PRD91, 034020 (2015);
Q. Wu , G. Li *et. al.*, Adv.High Energy Phys. 3729050

4th workshop on the XYZ particles, 北航, 2016年11月23-25日



Outline

- **Background**
- **Model and Numerical results**
- **Summary**



A summary of observed XYZ states

X. Liu, Chin. Sci. Bull. (2014) 59(29–30):3815–3830

A [1–5]	B [6–10]	C [11, 12]	D [13–15]	E [16–20]
$X(3872)$	$Y(4260)$	$X(3940)$	$X(3915)$	$Z_b(10610)$
$Y(3940)$	$Y(4008)$	$X(4160)$	$X(4350)$	$Z_b(10650)$
$Z^+(4430)$	$Y(4360)$	–	$Z(3930)$	$Z_c(3900)$
$Z^+(4051)$	$Y(4660)$	–	–	$Z_c(4025)$
$Z^+(4248)$	$Y(4630)$	–	–	$Z_c(4020)$
$Y(4140)$	–	–	–	$Z_c(3885)$
$Y(4274)$	X(3872): Belle, PRL91, 262001 (2003). Cited by 1228.			

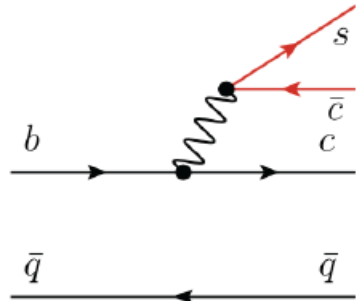




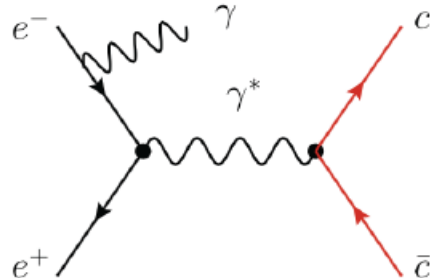
A summary of observed XYZ states

$X(3872)$
 $Y(3940)$
 $Z^+(4430)$
 $Z^+(4051)$
 $Z^+(4248)$
 $Y(4140)$
 $Y(4274)$

A: B meson decay

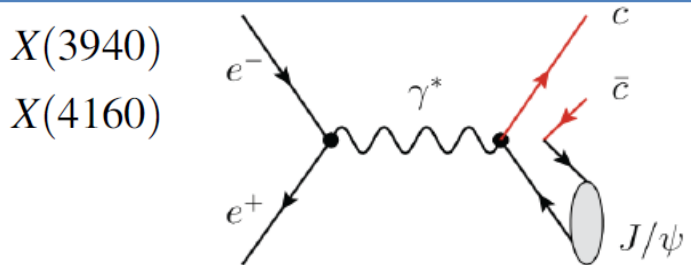


B: e^+e^- annihilation

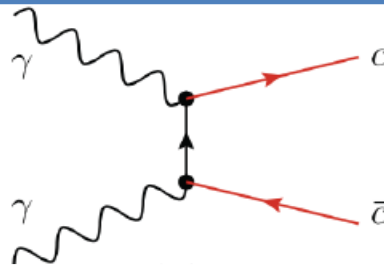


$Y(4260)$
 $Y(4008)$
 $Y(4360)$
 $Y(4660)$
 $Y(4630)$

C: The double charm production



D: $\gamma\gamma$ fusion process

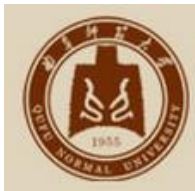


$X(3915)$
 $X(4350)$
 $Z(3930)$

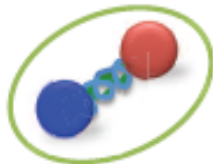
E: Hidden-charm/bottom dipion and open-charm/bottom decays of higher charmonia/bottomonia and charmoniumlike/bottomoniumlike states

X. Liu, Chin. Sci. Bull. (2014) 59(29–30):3815–3830

$Z_b(10610)$
 $Z_b(10650)$
 $Z_c(3900)$
 $Z_c(4025)$
 $Z_c(4020)$
 $Z_c(3885)$



Explanations of the XYZ states



Hybrid

⇒ Compact object with excited gluons and $Q\bar{Q}$

S.L. Zhu, PLB625(2005)212, E. Kou et al., PLB631(2005)164, F.E. Close et al., PLB628(2005)215, ...



Tetraquark

⇒ Compact object formed from Qq and $\bar{Q}\bar{q}$

L. Maiani et al., PRD89(2014)114010, L. Maiani et al., PRD87(2013)111102, ...



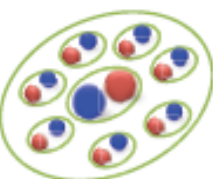
⇒ Compact object with color spin interaction

H.Hogaasen et. al., PRD73(2006)054013, F.Buccella et. al., EPJC49(2007)743, ...

Hadro-Quarkonium

⇒ Compact $Q\bar{Q}$ embedded in light quarks

M.B. Voloshin, Prog.Part.Nucl.Phys.61(2008)455, S. Dubynskiy et al., PLB666(2008)344, ...



Hadronic molecule

⇒ Extended object made of $Q\bar{q}$ and $\bar{Q}q$

N. A. Tornqvist, PLB590(2004)209, C.E. Thomas, PRD79(2008)034007, ...



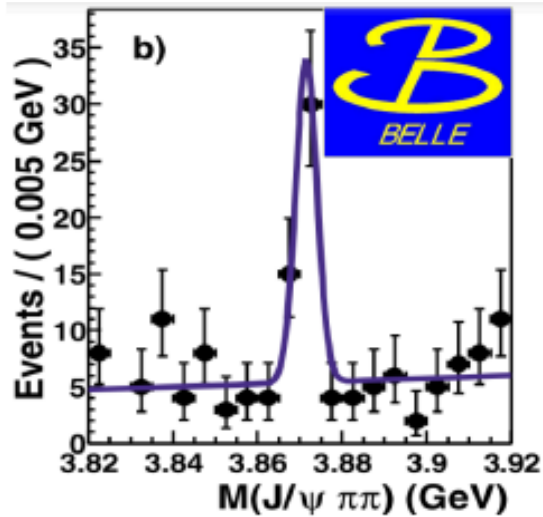


Some meson molecule candidates

States	Constituent	J^{PC}	Mass (GeV)
X(3872)	DD*	1^{++}	3.87169
Xb	BB*	1^{++}	?
Zc(3900)	DD*	1^{+-}	3.8887
Zc(4020)	D*D*	1^{+-}	4.0239
Zb(10610)	BB*	1^{+-}	10.6072
Zb(10650)	B*B*	1^{+-}	10.6522



X(3872)—best established



Discovered in $B^\pm \rightarrow K^\pm J/\psi \pi\pi$, mass extremely close to the $D^0 \bar{D}^{*0}$ threshold
 $M_X = (3871.69 \pm 0.17) \text{ MeV}$

$$M_{D^0} + M_{D^{*0}} - M_X = (0.12 \pm 0.19) \text{ MeV}$$

$$\Gamma < 1.2 \text{ MeV} \quad \text{Belle, PRD84(2011)052004}$$

$$J^{PC} = 1^{++} \quad \text{LHCb PRL110(2013)222001}$$

Belle, Babar, BESIII, CDF, CMS, D0, LHCb

normal $Q\bar{Q}$

hybrid states

tetraquarks

hadronic molecules

hadro-charmonia / hadro-bottomonia: heavy quarkonium bound inside light hadronic matter

S. Dubynskiy, M.B. Voloshin, PLB666(2008)344

.....



Conterpart of X(3872)—Xb states

Conterpart of X(3872): $J^{PC} = 1^{++}; I = 0$; BB* molecule?

Very Heavy: difficult to directly produce at e^+e^-

PHYSICAL REVIEW D 74, 017504 (2006)

Searching for the bottom counterparts of $X(3872)$ and $Y(4260)$ via $\pi^+\pi^-Y$

Wei-Shu Hou

Department of Physics, National Taiwan University, Taipei, Taiwan 10617, Republic Of China

(Received 5 June 2006; published 27 July 2006)

The $X(3872)$ and $Y(4260)$, among a host of charmoniumlike mesons, have rather unusual properties: the former has very small total width, the latter has large rate into $\pi^+\pi^-J/\psi$ channel. It would not be easy to settle between the many suggested explanations for their composition. We point out that discovering the bottom counterparts should shed much light on the issue. The narrow state can be searched for at the Tevatron via $p\bar{p} \rightarrow \pi^+\pi^-Y + X$, but the LHC should be much more promising. The state with large overlap with Y can be searched for at B factories via radiative return $e^+e^- \rightarrow \gamma_{ISR} + \pi^+\pi^-Y$ on $Y(5S)$, or by $e^+e^- \rightarrow \pi^+\pi^-Y$ direct scan.



Conterpart of X(3872)—Xb states

Conterpart of X(3872): $J^{PC} = 1^{++}; I = 0$; BB* molecule?

Very Heavy: difficult to directly produce at e^+e^-

G. Aad *et al.* [ATLAS Collaboration], Search for the Xb and other hidden-beauty states in the $\pi^+ \pi^-$ Upsilon(1S) channel at ATLAS, Phys. Lett. B740, 199 (2015).

S. Chatrchyan *et al.* [CMS Collaboration], Search for a new bottomonium state decaying to $\Upsilon(1S)\pi^+\pi^-$ in pp collisions at $\sqrt{s} = 8$ TeV, Phys. Lett. B 727, 57 (2013).

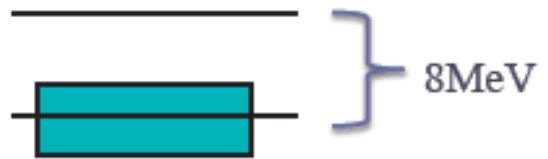
No evidence for Xb signal is found!



Conterpart of X(3872)--X_b states

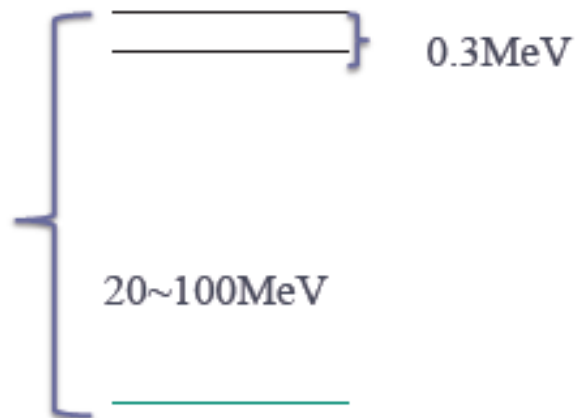
- $X(3872): M(D^+) + M(D^{*-}) = 3879.87 \pm 0.17 \text{ MeV}$
 $M(D^0) + M(D^{*0}) = 3871.8 \pm 0.17 \text{ MeV}$
 $M(X(3872)) = 3871.69 \pm 0.17 \text{ MeV}$

→ $X(3872) \rightarrow J/\psi \rho$ is large, isospin breaking



- $X_b: M(B^0) + M(B^{*0}) = 10604.8 \pm 0.57 \text{ MeV}$
 $M(B^+) + M(B^{*-}) = 10604.5 \pm 0.57 \text{ MeV}$
 $M(X_b) = 10504 \text{ MeV } 0911.2787$
 $10580 \text{ MeV } 1303.6608$

→ $X_b \rightarrow Y \rho$ may be suppressed by isospin.



$X_b \rightarrow \Upsilon(nS)\gamma, \chi_{bJ}\pi\pi, \Upsilon\omega$ should be of high priority.

G.Li, W.Wang, PLB733,100; G.Li, Z.Zhou, PRD91,034020.

Heavy-meson loops effects in the production and decays of ordinary states and exotic state candidates

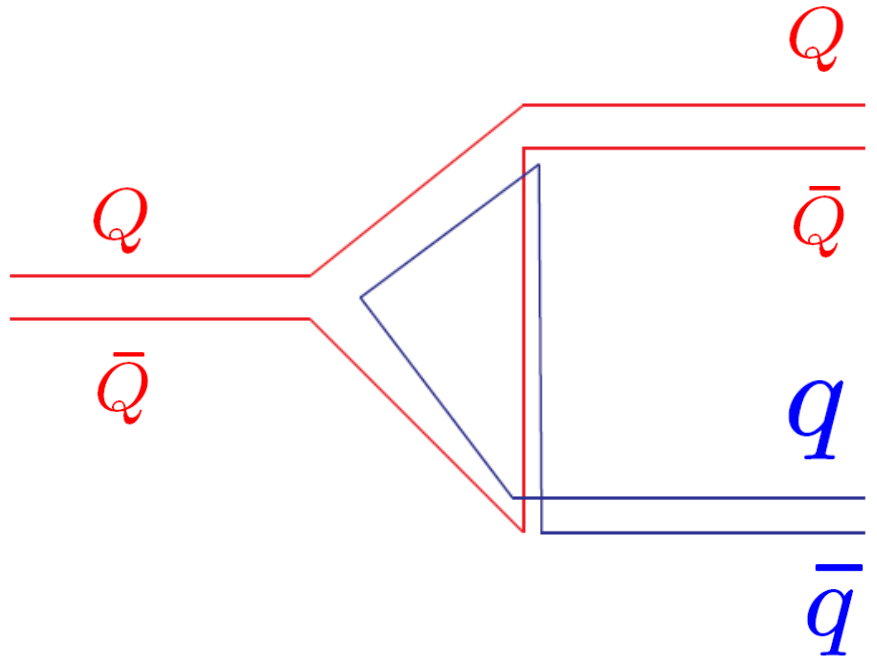


- ◆ Q. Wang, C. Hanhart and Q. Zhao, Phys. Rev. Lett. 111, 132003 (2013); F. -K. Guo, C. Hanhart, U. -G. Meißner, Q. Wang and Q. Zhao, Phys. Lett. B 725, 127 (2013); Q. Wang, C. Hanhart and Q. Zhao, Phys. Lett. B 725, no. 1-3, 106 (2013); M. Cleven, Q. Wang, F. -K. Guo, C. Hanhart, U. -G. Meißner and Q. Zhao, Phys. Rev. D 87, no. 7, 074006 (2013).
- ◆ D. -Y. Chen, X. Liu and T. Matsuki, Phys. Rev. D 84, 074032 (2011); D. -Y. Chen, X. Liu and T. Matsuki, arXiv:1208.2411 [hep-ph]; D. -Y. Chen, X. Liu and T. Matsuki, Phys. Rev. D 88, 036008 (2013); D. -Y. Chen, X. Liu and T. Matsuki, Phys. Rev. D 88, 014034 (2013); D. -Y. Chen and X. Liu, Phys. Rev. D 84, 094003 (2011).
- ◆ M. B. Voloshin, Phys. Rev. D 87, no. 7, 074011 (2013); M. B. Voloshin, Phys. Rev. D 84, 031502 (2011).
- ◆ A. E. Bondar, A. Garmash, A. I. Milstein, R. Mizuk and M. B. Voloshin, Phys. Rev. D 84, 054010 (2011).
- ◆ G. Li, F. -I. Shao, C. -W. Zhao and Q. Zhao, Phys. Rev. D 87, no. 3, 034020 (2013); X. -H. Liu and G. Li, Phys. Rev. D 88, 014013 (2013); G. Li and X. -H. Liu, Phys. Rev. D 88, 094008 (2013).

.....

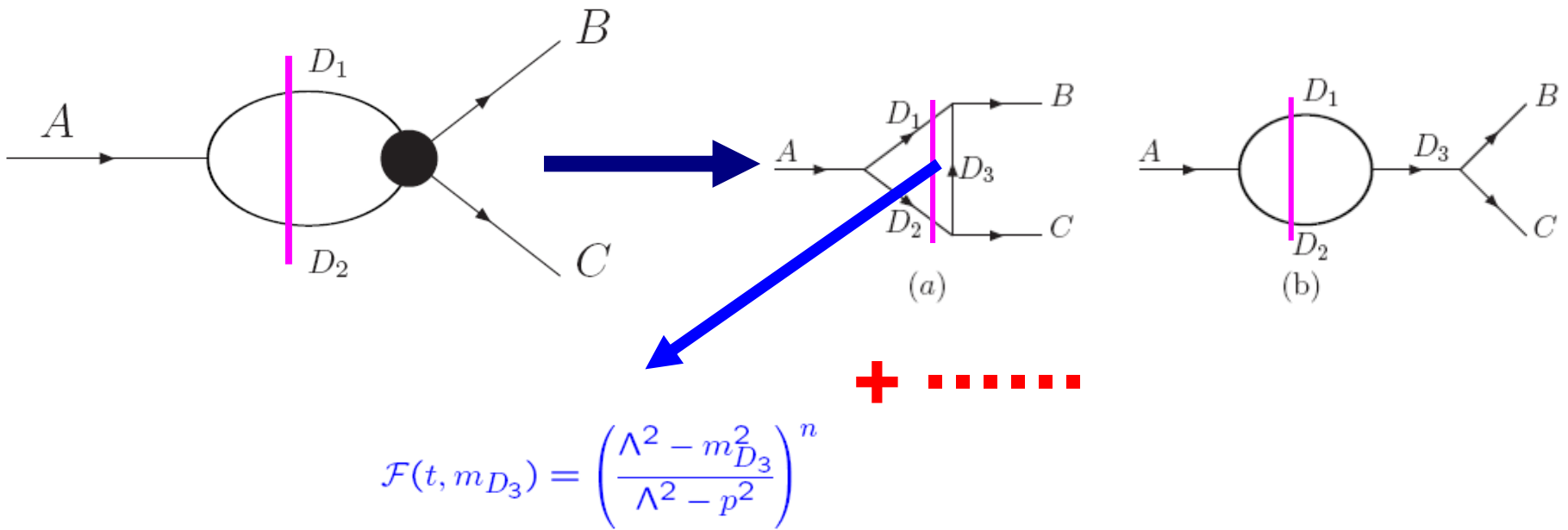


Quark-level descriptions of hadronic loop mechanism





Decomposition of intermediate meson loop transitions



$$X_b \rightarrow \Upsilon(nS)\gamma$$

G.Li, W. Wang, Phys. Lett. B733, 100.

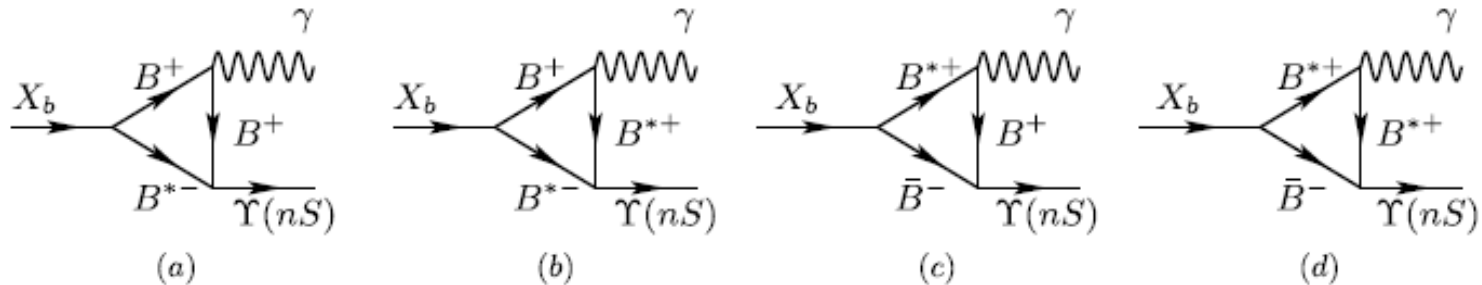


Fig. 1. Feynman diagrams for the radiative decays $X_b \rightarrow \gamma \Upsilon(nS)$ with the $B\bar{B}^*$ as the intermediate states.

Introduce form factors to
kill the divergence and
also compensate the off-
shell effects of
intermediate mesons

Monopole: $\mathcal{F}(m_2, q_2^2) \equiv \frac{\Lambda^2 - m_2^2}{\Lambda^2 - q_2^2}$

Dipole: $\mathcal{F}(m_2, q_2^2) \equiv \left(\frac{\Lambda^2 - m_2^2}{\Lambda^2 - q_2^2} \right)^2$

$$M_{fi} = \int \frac{d^4 q_2}{(2\pi)^4} \sum_{B^* \text{ pol.}} \frac{V_1 V_2 V_3}{a_1 a_2 a_3} \mathcal{F}(m_2, q_2^2)$$

$$\Lambda \equiv m_2 + \alpha \Lambda_{\text{QCD}}$$

$$\Lambda_{\text{QCD}} = 220 \text{ MeV}$$

Adopt the effective Lagrangian approach to do the calculation



$$\mathcal{L} = \frac{1}{2} X_{b\mu}^\dagger [x_1(B^{*0\mu} \bar{B}^0 - B^0 \bar{B}^{*0\mu}) + x_2(B^{*+\mu} B^- - B^+ B^{*-\mu})] + h.c.,$$

$$\begin{aligned}\mathcal{L}_{\Upsilon(nS)B^{(*)}B^{(*)}} = & ig_{\Upsilon BB} \Upsilon_\mu (\partial^\mu B \bar{B} - B \partial^\mu \bar{B}) - g_{\Upsilon B^* B} \varepsilon^{\mu\nu\alpha\beta} \partial_\mu \Upsilon_\nu (\partial_\alpha B_\beta^* \bar{B} + B \partial_\alpha \bar{B}_\beta^*) \\ & - ig_{\Upsilon B^* B^*} \{ \Upsilon^\mu (\partial_\mu B^{*\nu} \bar{B}_\nu^* - B^{*\nu} \partial_\mu \bar{B}_\nu^*) + (\partial_\mu \Upsilon_\nu B^{*\nu} - \Upsilon_\nu \partial_\mu B^{*\nu}) \bar{B}^{*\mu} \\ & + B^{*\mu} (\Upsilon^\nu \partial_\mu \bar{B}_\nu^* - \partial_\mu \Upsilon^\nu \bar{B}_\nu^*) \},\end{aligned}$$

$$\mathcal{L}_\gamma = \frac{e\beta Q_{ab}}{2} F^{\mu\nu} \text{Tr}[H_b^\dagger \sigma_{\mu\nu} H_a] + \frac{eQ'}{2m_Q} F^{\mu\nu} \text{Tr}[H_a^\dagger H_a \sigma_{\mu\nu}],$$

P. Colangelo, F. De Fazio, T.N. Pham, Phys. Rev. D 69 (2004) 054023, arXiv:hep-ph/0310084.

R. Casalbuoni, A. Deandrea, N. Di Bartolomeo, R. Gatto, F. Feruglio, G. Nardulli, Phys. Rep. 281 (1997) 145, arXiv:hep-ph/9605342.

J. Hu, T. Mehen, Phys. Rev. D 73 (2006) 054003, arXiv:hep-ph/0511321.

J.F. Amundson, C.G. Boyd, E.E. Jenkins, M.E. Luke, A.V. Manohar, J.L. Rosner, M.J. Savage, M.B. Wise, Phys. Lett. B 296 (1992) 415, arXiv:hep-ph/9209241.



Coupling constants determination

$$g_{\gamma BB} = 2g_2 \sqrt{m_B} m_B , \quad g_{\gamma B^* B} = \frac{g_{\gamma BB}}{\sqrt{m_B m_{B^*}}} , \quad g_{\gamma B^* B^*} = g_{\gamma B^* B} \sqrt{\frac{m_{B^*}}{m_B}} m_{B^*} ,$$

$$\chi_i^2 \equiv 16\pi (m_B + m_{B^*})^2 c_i^2 \sqrt{\frac{2E_{X_b}}{\mu}}$$

$$E_{X_b} = m_B + m_{B^*} - m_{X_b}$$

$$c_i = 1/\sqrt{2}, \mu = m_B m_{B^*} / (m_B + m_{B^*})$$

$$g_n = \sqrt{m_{\gamma(nS)}} / (2m_B f_{\gamma(nS)}) \quad Q = \text{diag}\{2/3, -1/3, -1/3\} \quad \beta \simeq 3.0 \text{ GeV}^{-1}$$

P. Colangelo, F. De Fazio, T.N. Pham, Phys. Rev. D 69 (2004) 054023, arXiv:hep-ph/0310084.

R. Casalbuoni, A. Deandrea, N. Di Bartolomeo, R. Gatto, F. Feruglio, G. Nardulli, Phys. Rep. 281 (1997) 145, arXiv:hep-ph/9605342.

J. Hu, T. Mehen, Phys. Rev. D 73 (2006) 054003, arXiv:hep-ph/0511321.

J.F. Amundson, C.G. Boyd, E.E. Jenkins, M.E. Luke, A.V. Manohar, J.L. Rosner, M.J. Savage, M.B. Wise, Phys. Lett. B 296 (1992) 415, arXiv:hep-ph/9209241.

F.-K. Guo, C. Hanhart, U.-G. Meißner, Q. Wang, Q. Zhao, Phys. Lett. B 725 (2013) 127, arXiv:1306.3096 [hep-ph].

S. Weinberg, Phys. Rev. 137 (1965) B672.

V. Baru, J. Haidenbauer, C. Hanhart, Y. Kalashnikova, A.E. Kudryavtsev, Phys. Lett. B 586 (2004) 53, arXiv:hep-ph/0308129.



Numerical results

The Xb Mass Prediction:

Tetraquark calculation: 10504 MeV

A. Ali, C. Hambrock, I. Ahmed and M. J. Aslam, Phys. Lett. B684, 28 (2010)

Hadronic molecular calculations: (10580^{+9}_{-8}) MeV

F. K. Guo, C. Hidalgo-Duque, J. Nieves, M,P. Valderrama, Phys. Rev. D88, 054007 (2013).



Numerical results

Predicted partial widths (in unit of keV) of the X_b decays. The parameter in the form factor is chosen as $\alpha = 2.0$ and $\alpha = 3.0$.

	$X_b \rightarrow \gamma \Upsilon(1S)$		$X_b \rightarrow \gamma \Upsilon(2S)$		$X_b \rightarrow \gamma \Upsilon(3S)$	
Dipole form factor	$\alpha = 2.0$	$\alpha = 3.0$	$\alpha = 2.0$	$\alpha = 3.0$	$\alpha = 2.0$	$\alpha = 3.0$
$E_{X_b} = 1$ MeV	0.12	0.41	0.34	0.96	0.22	0.46
$E_{X_b} = 2$ MeV	0.19	0.62	0.42	1.18	0.28	0.57
$E_{X_b} = 5$ MeV	0.28	0.92	0.53	1.53	0.33	0.70
$E_{X_b} = 20$ MeV	0.36	1.20	0.66	1.96	0.30	0.66
Monopole form factor	$\alpha = 2.0$	$\alpha = 3.0$	$\alpha = 2.0$	$\alpha = 3.0$	$\alpha = 2.0$	$\alpha = 3.0$
$E_{X_b} = 1$ MeV	0.02	0.06	0.05	0.11	0.03	0.06
$E_{X_b} = 2$ MeV	0.04	0.08	0.07	0.16	0.04	0.08
$E_{X_b} = 5$ MeV	0.06	0.13	0.12	0.26	0.07	0.12
$E_{X_b} = 20$ MeV	0.13	0.30	0.26	0.56	0.12	0.22

The predicted widths are about 1 keV.

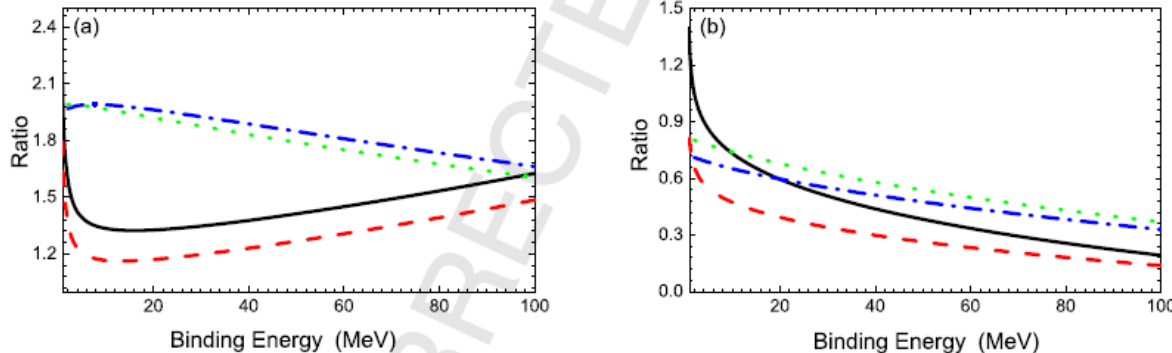


Fig. 4. (a) The ratio R_1 defined in Eq. (12) in terms of the E_{X_b} , with dipole form factors $\alpha = 2.0$ (solid line) and $\alpha = 3.0$ (dashed line), and monopole form factors with $\alpha = 2.0$ (dotted lines) and $\alpha = 3.0$ (dash-dotted lines), respectively. (b) The same notation with (a) except for R_2 defined in Eq. (12).

$$R_1 = \frac{\Gamma(X_b \rightarrow \gamma \Upsilon(2S))}{\Gamma(X_b \rightarrow \gamma \Upsilon(1S))}, \quad R_2 = \frac{\Gamma(X_b \rightarrow \gamma \Upsilon(3S))}{\Gamma(X_b \rightarrow \gamma \Upsilon(1S))},$$

The ratio R are not sensitive to the long-range structure of the X_b .

$X_b \rightarrow \Upsilon(1S)\omega$

G. Li, Z. Zhou, Phys. Rev. D91, 034020.

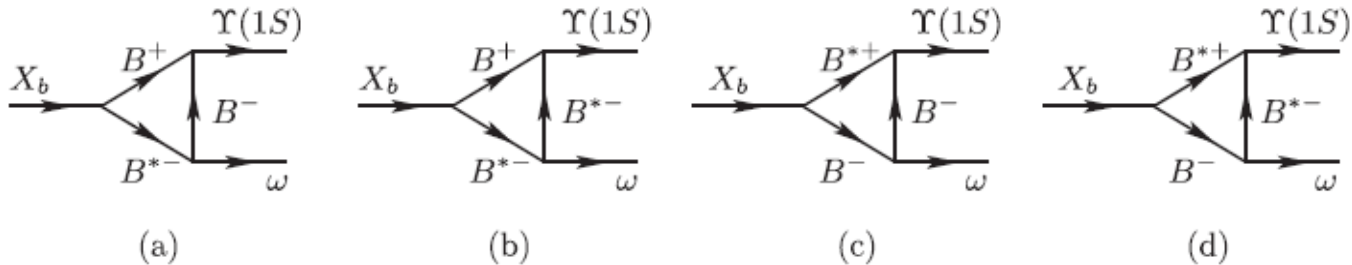


FIG. 1. Feynman diagrams for $X_b \rightarrow \Upsilon(1S)\omega$ with the $B\bar{B}^*$ as the intermediate states.

$$\mathcal{L} = \frac{1}{2} X_{b\mu}^\dagger [x_1(B^{*0\mu}\bar{B}^0 - B^0\bar{B}^{*0\mu}) + x_2(B^{*+\mu}B^- - B^+B^{*-\mu})] + H.c.$$

$$\begin{aligned} \mathcal{L}_{\Upsilon(1S)B^{(*)}B^{(*)}} &= ig_{\Upsilon BB} \Upsilon_\mu (\partial^\mu B\bar{B} - B\partial^\mu \bar{B}) - g_{\Upsilon B^*B} \epsilon_{\mu\nu\alpha\beta} \partial^\mu \Upsilon^\nu (\partial^\alpha B^{*\beta}\bar{B} + B\partial^\alpha \bar{B}^{*\beta}) \\ &\quad - ig_{\Upsilon B^*B^*} \left\{ \Upsilon^\mu (\partial_\mu B^{*\nu}\bar{B}_\nu^* - B^{*\nu}\partial_\mu \bar{B}_\nu^*) + (\partial_\mu \Upsilon_\nu B^{*\nu} - \Upsilon_\nu \partial_\mu B^{*\nu}) \bar{B}^{*\mu} \right. \\ &\quad \left. + B^{*\mu} (\Upsilon^\nu \partial_\mu \bar{B}_\nu^* - \partial_\mu \Upsilon_\nu \bar{B}_\nu^*) \right\}, \end{aligned}$$

$$\begin{aligned} \mathcal{L} &= -ig_{BBV} \mathcal{B}_i^\dagger \overset{\leftrightarrow}{\partial}_\mu \mathcal{B}_j^j (\mathcal{V}^\mu)_j^i - 2f_{B^*B\mathcal{V}} \epsilon_{\mu\nu\alpha\beta} (\partial^\mu \mathcal{V}^\nu)_j^i (\mathcal{B}_i^\dagger \overset{\leftrightarrow}{\partial}^\alpha \mathcal{B}^{*j\beta} - \mathcal{B}_i^{*\beta\dagger} \overset{\leftrightarrow}{\partial}^\alpha \mathcal{B}_j^j) + ig_{B^*B^*\mathcal{V}} \mathcal{B}_i^{*\nu\dagger} \overset{\leftrightarrow}{\partial}_\mu \mathcal{B}_\nu^j (\mathcal{V}^\mu)_j^i \\ &\quad + 4if_{B^*B^*\mathcal{V}} \mathcal{B}_{i\mu}^{*\dagger} (\partial^\mu \mathcal{V}^\nu - \partial^\nu \mathcal{V}^\mu)_j^i \mathcal{B}_\nu^{*j}, \end{aligned}$$



Coupling constants determinations

$$g_{\Upsilon(1S)BB} = 2g_1 \sqrt{m_{\Upsilon(1S)} m_B}, \quad g_{\Upsilon(1S)B^*B} = \frac{g_{\Upsilon(1S)BB}}{\sqrt{m_B m_{B^*}}}, \quad g_{\Upsilon(1S)B^*B^*} = g_{\Upsilon(1S)B^*B} \sqrt{\frac{m_{B^*}}{m_B}} m_{B^*}$$
$$x_i^2 \equiv 16\pi(m_B + m_{B^*})^2 c_i^2 \sqrt{\frac{2E_{X_b}}{\mu}} \quad g_{\mathcal{B}\mathcal{B}\mathcal{V}} = g_{\mathcal{B}^*\mathcal{B}^*\mathcal{V}} = \frac{\beta g_V}{\sqrt{2}}, \quad f_{\mathcal{B}^*\mathcal{B}\mathcal{V}} = \frac{f_{\mathcal{B}^*\mathcal{B}^*\mathcal{V}}}{m_{\mathcal{B}^*}} = \frac{\lambda g_V}{\sqrt{2}}$$

$$g_1 = \sqrt{m_{\Upsilon(1S)}} / (2m_B f_{\Upsilon(1S)}) \quad f_{\Upsilon(1S)} = 715.2 \text{ MeV}$$

$$\beta = 0.9, \lambda = 0.56 \text{ GeV}^{-1} \quad g_V = m_\rho / f_\pi$$

S. Weinberg, [Phys. Rev. 137, B672 \(1965\)](#).

V. Baru, J. Haidenbauer, C. Hanhart, Y. Kalashnikova, and A. E. Kudryavtsev, [Phys. Lett. B 586, 53 \(2004\)](#).

P. Colangelo, F. De Fazio, and T. N. Pham, [Phys. Rev. D 69, 054023 \(2004\)](#).

R. Casalbuoni, A. Deandrea, N. Di Bartolomeo, R. Gatto, F. Feruglio, and G. Nardulli, [Phys. Rept. 281, 145 \(1997\)](#).

C. Isola, M. Ladisa, G. Nardulli, and P. Santorelli, [Phys. Rev. D 68, 114001 \(2003\)](#).

D. Becirevic, B. Blossier, E. Chang, and B. Haas, [Phys. Lett. B 679, 231 \(2009\)](#).



Numerical results for $X_b \rightarrow \Upsilon(1S)\omega$

TABLE I. Predicted partial widths (in units of keV) of the X_b decays. The parameter in the form factor is chosen as $\alpha = 2.0$, 2.5, and 3.0, respectively. The units of the binding energy parameters E_{X_b} in column 1 are all MeV.

Dipole form factor	$\alpha = 2.0$	$\alpha = 2.5$	$\alpha = 3.0$
$E_{X_b} = 1$ MeV	4.03	8.55	15.53
$E_{X_b} = 5$ MeV	8.38	17.84	32.51
$E_{X_b} = 10$ MeV	11.17	23.84	43.56
$E_{X_b} = 25$ MeV	15.12	33.30	61.10
$E_{X_b} = 50$ MeV	18.63	40.14	73.96
$E_{X_b} = 100$ MeV	20.02	43.34	80.22

The widths are about tens of keVs, which indicate a sizeable branching ratios.

No significant signal for $X_b \rightarrow \Upsilon(1S)\omega$ has been seen by the Belle Collaboration.

X. H. He et al. [Belle Collaboration], Phys. Rev. Lett. 113, 142001 (2014)



Detecting the structure of Xb

Based on the Xb being an S-wave BB* molecule ansatz

Xb molecule picture: $S_H \otimes S_L = 1_H^{--} \otimes 1_L^{--}$

Xb tetraquark picture: S_H can be 0 or 1

The processes $X_b \rightarrow \Upsilon(nS)\gamma, \Upsilon(1S)\omega$ are not sensitive to the BB* wave function at the long distance, but rather they are determined by the short distance part of the Xb.

The process $X_b \rightarrow B\bar{B}\gamma$ can be used to probe the long structure of Xb.



$\Upsilon(5S, 6S) \rightarrow X_b \gamma$

Q. Wu, G. Li, et al., Adv.High Energy Phys. 3729050 (2016) .

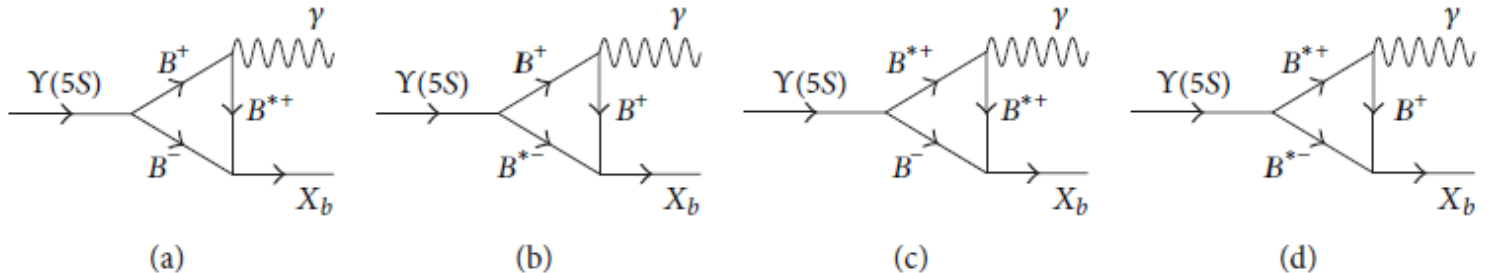


FIGURE 1: Feynman diagrams for X_b production in $\Upsilon(5S) \rightarrow \gamma X_b$ under $B\bar{B}^*$ meson loop effects.

$$\mathcal{L} = \frac{1}{2} X_{b\mu}^\dagger [x_1(B^{*0\mu} \bar{B}^0 - B^0 \bar{B}^{*0\mu}) + x_2(B^{*\mu} B^- - B^+ B^{*-\mu})] + h.c.,$$

$$\begin{aligned} \mathcal{L}_{\Upsilon(nS)B^{(*)}B^{(*)}} &= ig_{\Upsilon BB} \Upsilon_\mu (\partial^\mu B \bar{B} - B \partial^\mu \bar{B}) - g_{\Upsilon B^* B} \varepsilon^{\mu\nu\alpha\beta} \partial_\mu \Upsilon_\nu (\partial_\alpha B_\beta^* \bar{B} + B \partial_\alpha \bar{B}_\beta^*) \\ &\quad - ig_{\Upsilon B^* B^*} \{ \Upsilon^\mu (\partial_\mu B^{*\nu} \bar{B}_\nu^* - B^{*\nu} \partial_\mu \bar{B}_\nu^*) + (\partial_\mu \Upsilon_\nu B^{*\nu} - \Upsilon_\nu \partial_\mu B^{*\nu}) \bar{B}^{*\mu} \\ &\quad + B^{*\mu} (\Upsilon^\nu \partial_\mu \bar{B}_\nu^* - \partial_\mu \Upsilon^\nu \bar{B}_\nu^*) \}, \end{aligned}$$

$$\mathcal{L}_\gamma = \frac{e\beta Q_{ab}}{2} F^{\mu\nu} \text{Tr}[H_b^\dagger \sigma_{\mu\nu} H_a] + \frac{eQ'}{2m_Q} F^{\mu\nu} \text{Tr}[H_a^\dagger H_a \sigma_{\mu\nu}],$$



$$\Upsilon(5S, 6S) \rightarrow X_b \gamma$$

TABLE 1: The coupling constants of $\Upsilon(5S)$ interacting with $B^{(*)}\bar{B}^{(*)}$. Here, we list the corresponding branching ratios of $\Upsilon(5S) \rightarrow B^{(*)}\bar{B}^{(*)}$.

Final state	\mathcal{B} (%)	Coupling
$B\bar{B}$	5.5	1.76
$B_s\bar{B}_s$	0.5	0.96
$B\bar{B}^*$ + c.c.	13.7	0.14 GeV^{-1}
$B_s\bar{B}_s^*$ + c.c.	1.35	0.10 GeV^{-1}
$B^*\bar{B}^*$	38.1	2.22
$B_s^*\bar{B}_s^*$	17.6	5.07

Numerical results for $\Upsilon(5S, 6S) \rightarrow \gamma X_b$

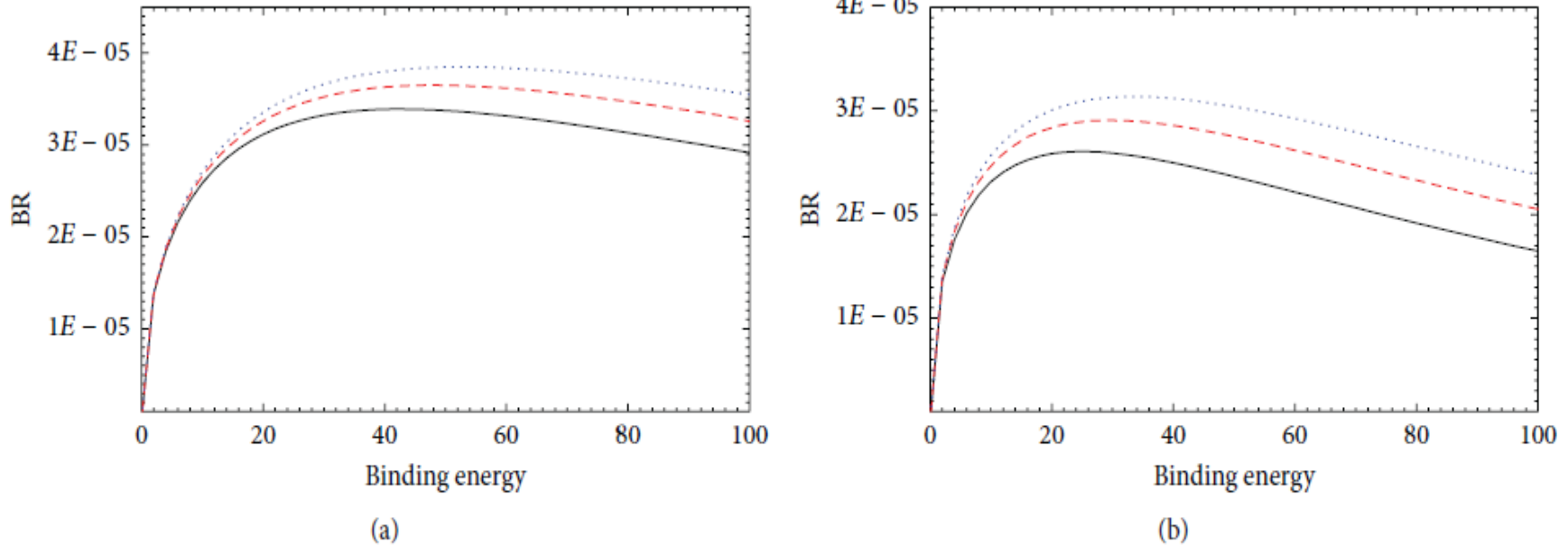


FIGURE 2: (a) The dependence of the branching ratios of $\Upsilon(5S) \rightarrow \gamma X_b$ on ϵ_{X_b} using monopole form factors with $\alpha = 2.0$ (solid lines), $\alpha = 2.5$ (dashed lines), and $\alpha = 3.0$ (dotted lines), respectively. (b) The dependence of the branching ratios of $\Upsilon(5S) \rightarrow \gamma X_b$ on ϵ_{X_b} using dipole form factors with $\alpha = 2.0$ (solid lines), $\alpha = 2.5$ (dashed lines), and $\alpha = 3.0$ (dotted lines), respectively. The results with binding energy up to 100 MeV might make the molecular state assumption inaccurate.

The behavior of the branching ratios is relatively sensitive at small ϵ_{X_b} , while it becomes smooth at large ϵ_{X_b} .

Numerical results for $\Upsilon(5S,6S) \rightarrow \gamma X_b$

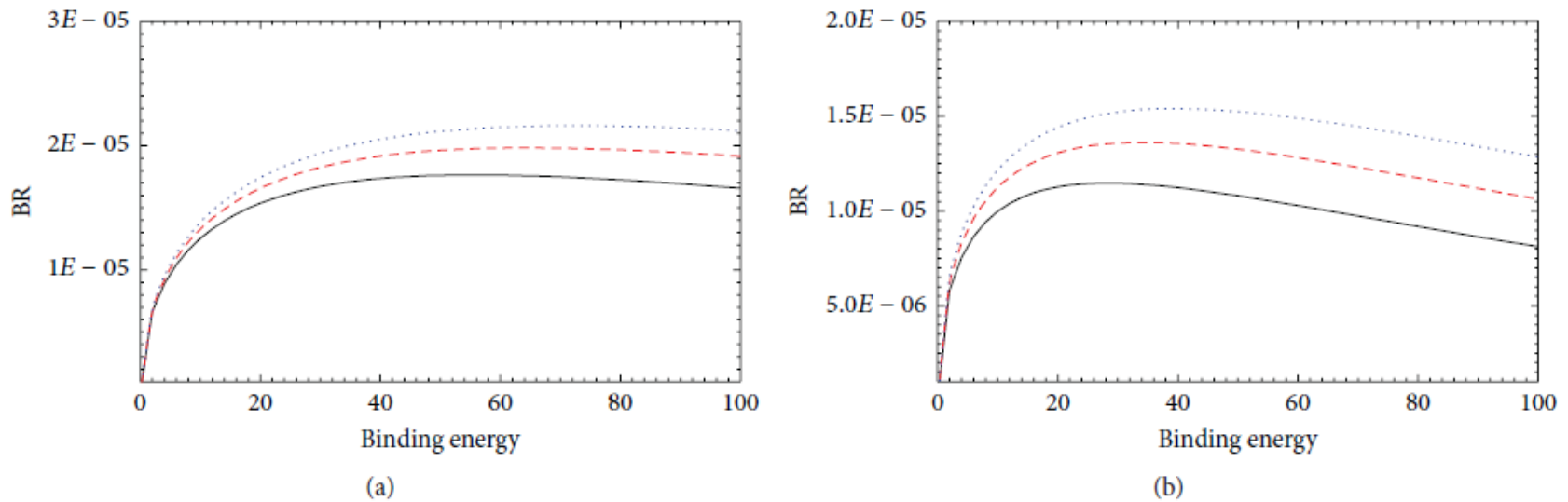


FIGURE 3: (a) The dependence of the branching ratios of $\Upsilon(6S) \rightarrow \gamma X_b$ on ϵ_{X_b} using monopole form factors with $\alpha = 2.0$ (solid lines), $\alpha = 2.5$ (dashed lines), and $\alpha = 3.0$ (dotted lines), respectively. (b) The dependence of the branching ratios of $\Upsilon(6S) \rightarrow \gamma X_b$ on ϵ_{X_b} using dipole form factors with $\alpha = 2.0$ (solid lines), $\alpha = 2.5$ (dashed lines), and $\alpha = 3.0$ (dotted lines), respectively. The results with binding energy up to 100 MeV might make the molecular state assumption inaccurate.



Numerical results for $\Upsilon(5S, 6S) \rightarrow \gamma X_b$

TABLE 2: Predicted branching ratios for $\Upsilon(5S) \rightarrow \gamma X_b$. The parameter in the form factor is chosen as $\alpha = 2.0, 2.5$, and 3.0 . The last column is the calculated branching ratios in NREFT approach.

Binding energy	Monopole form factor			Dipole form factor			NREFT
	$\alpha = 2.0$	$\alpha = 2.5$	$\alpha = 3.0$	$\alpha = 2.0$	$\alpha = 2.5$	$\alpha = 3.0$	
$\epsilon_{X_b} = 5 \text{ MeV}$	2.02×10^{-5}	2.06×10^{-5}	2.08×10^{-5}	1.90×10^{-5}	1.99×10^{-5}	2.04×10^{-5}	1.52×10^{-6}
$\epsilon_{X_b} = 10 \text{ MeV}$	2.58×10^{-5}	2.66×10^{-5}	2.71×10^{-5}	2.32×10^{-5}	2.47×10^{-5}	2.57×10^{-5}	2.12×10^{-6}
$\epsilon_{X_b} = 25 \text{ MeV}$	3.24×10^{-5}	3.42×10^{-5}	3.54×10^{-5}	2.61×10^{-5}	2.90×10^{-5}	3.09×10^{-5}	3.88×10^{-6}
$\epsilon_{X_b} = 50 \text{ MeV}$	3.37×10^{-5}	3.65×10^{-5}	3.85×10^{-5}	2.37×10^{-5}	2.75×10^{-5}	3.04×10^{-5}	6.41×10^{-6}
$\epsilon_{X_b} = 100 \text{ MeV}$	2.91×10^{-5}	3.27×10^{-5}	3.54×10^{-5}	1.65×10^{-5}	2.05×10^{-5}	2.38×10^{-5}	1.20×10^{-5}

TABLE 3: Predicted branching ratios for $\Upsilon(6S) \rightarrow \gamma X_b$. The parameter in the form factor is chosen as $\alpha = 2.0, 2.5$, and 3.0 . The last column is the calculated branching ratios in NREFT approach.

Binding energy	Monopole form factor			Dipole form factor			NREFT
	$\alpha = 2.0$	$\alpha = 2.5$	$\alpha = 3.0$	$\alpha = 2.0$	$\alpha = 2.5$	$\alpha = 3.0$	
$\epsilon_{X_b} = 5 \text{ MeV}$	9.71×10^{-6}	1.02×10^{-5}	1.05×10^{-5}	8.16×10^{-6}	9.04×10^{-6}	9.63×10^{-6}	3.38×10^{-6}
$\epsilon_{X_b} = 10 \text{ MeV}$	1.25×10^{-5}	1.33×10^{-5}	1.38×10^{-5}	9.97×10^{-6}	1.13×10^{-5}	1.22×10^{-5}	4.89×10^{-6}
$\epsilon_{X_b} = 25 \text{ MeV}$	1.62×10^{-5}	1.76×10^{-5}	1.85×10^{-5}	1.14×10^{-5}	1.34×10^{-5}	1.49×10^{-5}	8.27×10^{-6}
$\epsilon_{X_b} = 50 \text{ MeV}$	1.76×10^{-5}	1.96×10^{-5}	2.12×10^{-5}	1.08×10^{-5}	1.32×10^{-5}	1.52×10^{-5}	1.30×10^{-5}
$\epsilon_{X_b} = 100 \text{ MeV}$	1.66×10^{-5}	1.92×10^{-5}	2.12×10^{-5}	8.12×10^{-6}	1.06×10^{-5}	1.28×10^{-5}	2.24×10^{-5}



Numerical results for $\Upsilon(5S,6S) \rightarrow \gamma X_b$

At the same cutoff parameter, the predicted rates for $\Upsilon(6S) \rightarrow \gamma X_b$ are a factor of 2–3 smaller than the corresponding rates for $\Upsilon(5S) \rightarrow \gamma X_b$.

Except for the largest binding energy 100MeV, the NREFT predictions of $\Upsilon(5S) \rightarrow \gamma X_b$ are about 1 order of magnitude smaller than the ELA results at the commonly accepted range. For $\Upsilon(6S) \rightarrow \gamma X_b$, the NREFT predictions are several times smaller than the ELA results in small binding energy range, while the predictions of these two methods are comparable at large binding energy. These differences may give some sense of the theoretical uncertainties for the predicted rates and indicate the viability of our model to some extent.



Summary

The widths of $X_b \rightarrow \Upsilon(nS)\gamma$, $\Upsilon(1S)\omega$ are about 1 keV and tens of keVs, respectively, which corresponds to sizeable branching ratios.

The sizeable production ratios of $\Upsilon(5S,6S) \rightarrow \gamma X_b$ may be accessible at the future experiments like forthcoming BelleII,

Heavy meson loops effects play an important role in the decays of exotic states, especially when the initial state mass are close to the intermediate meson pair thresholds.

The discrimination of a compact multiquark configuration and a loosely bound hadronic molecule is an important aspects in the study of exotics.

Thanks for your attention !